

# The lymphangiogenesis inhibitor esVEGFR-2 in human embryos: expression in sympatho-adrenal tissues and differentiation-induced up-regulation in neuroblastoma

Jürgen Becker<sup>1</sup>, Johanna Fröhlich<sup>1</sup>, Jan Hansen<sup>1</sup>, Christina Zelent<sup>1</sup>, Christina Perske<sup>2</sup> and Jörg Wilting<sup>1</sup>

<sup>1</sup>Center of Anatomy, Department of Anatomy and Cell Biology and

<sup>2</sup>Department of Pathology, University Medicine Goettingen, Goettingen, Germany

**Summary.** Tumour-induced hem- and lymphangiogenesis are frequently associated with tumour progression. Vascular Endothelial Growth Factor-C (VEGF-C) is a potent inducer of lymphangiogenesis, while the endogenous soluble splice-variant of VEGF receptor-2, esVEGFR-2, acts as a natural inhibitor. Previously we have shown down-regulation of esVEGFR-2 mRNA in progressed stages of neuroblastoma (NB), a tumour derived from sympatho-adrenal precursor cells. Here we studied the immunolocalization of esVEGFR-2 in human embryos, infantile adrenal gland and primary NB. We also quantified esVEGFR-2 mRNA in NB cell lines after differentiation-induction by all-trans retinoic acid (ATRA). By immunoperoxidase staining we observed expression of esVEGFR-2 in both the sympathetic trunk and the adrenal medulla. Additionally, esVEGFR-2 was found in spinal ganglia, floor plate of the neural tube, choroid plexus, notochord, arterial endothelium, skeletal muscle, epidermis and gut epithelium. Developing and circulating leukocytes showed the strongest signal. In NB, esVEGFR-2 was considerably stronger in differentiating low grade tumours with neuronal phenotype than in undifferentiated lesions. Differentiation-induction of the NB cell line SMS-Kan with 5-10  $\mu$ M ATRA resulted in a significant increase of esVEGFR-2 mRNA after 6, 9 and 12 days. We show that esVEGFR-2 is widely expressed in embryonic tissues. Especially, the adrenal medulla and circulating leukocytes seem to be potent inhibitors of lymphangiogenesis. We provide additional evidence for a role of esVEGFR-2 in NB. Thereby, high levels of esVEGFR-2 correlate with a more differentiated phenotype, and may inhibit tumour progression by

inhibition of lymphangiogenesis.

**Key words:** Metastasis, Adrenal medulla, Lymphangiogenesis, ATRA, Differentiation

## Introduction

By the end of the 20th century, tumour-induced lymphangiogenesis was considered to be nonexistent (Folkman, 1996). Then, a new member of the Vascular Endothelial Growth Factor (VEGF) family was detected, named VEGF-C, which was found to induce lymphangiogenesis in chicken and mouse (Jeltsch et al., 1997; Oh et al., 1997). Tumour-induced lymphangiogenesis was observed in VEGF-C-expressing experimental tumours on the chicken chorioallantoic membrane (Papoutsis et al., 2000), and a positive correlation between tumour lymphangiogenesis and the formation of lymph node metastases was described in mice (Karpanen et al., 2001; Skobe et al., 2001; Stacker et al., 2001). In numerous tumours of the human, a positive correlation between the expression of the lymphangiogenic growth factors VEGF-C or VEGF-D and the lymphogenic spread of tumour cells has been found. However, in some tumours that disseminate via lymphatics such a correlation could not be observed (Pepper et al., 2003). It is likely that the balance between lymphangiogenic activators and inhibitors is crucial for the development of normal lymphatics.

Recently, an endogenous secreted splice variant of VEGF receptor-2, esVEGFR-2, was shown to inhibit lymphangiogenesis in the embryonic development of the dermis, the cornea and in corneal wounds. EsVEGFR-2 results from the partial retention of an intron 13 motif with in-frame termination at 39 (mouse) and 48 (human) nucleotides downstream from the exon 13-intron 13

boundary in the mature mRNA (Albuquerque et al., 2009). To differentiate esVEGFR-2 from soluble VEGFR-2, which may also be derived by proteolytic shedding from the cell surface (Roeckl et al., 1998; Ebos et al., 2004), we included the term 'endogenous' in the name, as was done in a recent study (Shibata et al., 2010). EsVEGFR-2 binds VEGF-C, but not VEGF-A, inhibits VEGF-C-induced phosphorylation of VEGFR-3, and reduces VEGF-C-induced proliferation of human lymphangioma endothelial cells (Albuquerque et al., 2009). Knock-out of VEGFR-2 in the corneal epithelium results in intra-corneal lymphangiogenesis of newborn mice. Knock-out in the epidermis induces hyperplasia of dermal lymphatics. There seem to be overlapping expression patterns of esVEGFR-2 in mice and humans. In both species, esVEGFR-2 is expressed in the epidermis, the corneal epithelium and in blood vascular endothelial cells (Pavlakovic et al., 2010).

Neuroblastoma (NB) is a solid childhood tumour derived from neural crest cells that form the sympathetic ganglia and the adrenal medulla (Weiss et al., 1997). Some years ago, the existence of lymphatics in NB was proven by immunohistological studies with D2-40 (anti-podoplanin) antibodies, and the expression of the lymphangiogenic growth factors VEGF-C and VEGF-D was found in a subset of these tumors (Lagodny et al., 2007). We have recently shown that the expression of esVEGFR-2 mRNA is high in NB of low stages, and significantly down-regulated in progressed NB (Becker et al., 2010). High vascularity is characteristic for the progressed NB stages (Meitar et al., 1996; Rossler et al., 2008). Importantly, lymph node involvement is a major criterion for the clinical staging of NB. Stage 1 characterizes localized disease without lymphatic involvement. Stages 2B and 3 mostly show involvement of loco-regional (ipsi- or contralateral) lymph nodes. Stage 4 NB has distant metastases into lymph nodes, bone marrow, liver and other organs. There is an enormous heterogeneity of NB, both morphologically and biologically. NB presents a high rate of spontaneous differentiation into benign ganglioneuroma. The presence of differentiating neuroblasts, cells with nuclear and cytoplasmic enlargement, is considered as a sign of tumor maturation (Tornoczky et al., 2007). This fact is widely recognized and results in a "wait and see" strategy for low-grade tumours.

Since our previous work has demonstrated the down-regulation of esVEGFR-2 mRNA in progressed NB stages, we were now interested in studying the localization of the protein, and to see if its expression correlates with development and differentiation. We studied immunolocalization of esVEGFR-2 in human embryos, fetuses and infants. In the embryos, we studied all organs, which were present in the sections, but paid special attention to sympatho-adrenal tissues. As the adrenal medulla is a major source of NB, we also studied normal adrenal gland of infants. Furthermore, we performed immunostaining with anti-esVEGFR-2 antibodies on undifferentiated and differentiating NB.

The effects of differentiation on esVEGFR-2 expression were then studied *in vitro* by the use of the differentiation-inducing agent all-trans retinoic acid (ATRA) (Reynolds et al., 2003). Here we show that esVEGFR-2 is expressed in a number of different tissues, especially high in leukocytes and adrenal medulla. It is high in differentiating but low in undifferentiated NB, which supports the assumption that the expression of esVEGFR2 is an important feature of normally developing sympathetic neuroblasts. The balance between lymphangiogenic activators and inhibitors may affect the clinical behaviour of NB.

## Materials and methods

### Human embryos and fetuses

Human embryos and fetuses (each three from gestational week 8 and week 10/11) were obtained from legal abortions and collected with the informed consent of the women according to the regulations of the Ethics Committee of the University Medicine Goettingen (application 6/1/04). The age of the embryos and fetuses was determined by an experienced embryologist from histological data according to the Carnegie stages (O'Rahilly and Müller, 1996). No abnormalities or signs of autolysis were noted in the specimens.

### Primary neuroblastomas

Paraffin sections of primary NB (n=15) were kindly provided by the Tumourbank of the German Neuroblastoma Studies Group (Drs. F. Berthold, B. Hero, J. Theissen) and by the Department of Pathology, University Medicine Goettingen (Head: Prof. H.-J. Radzun). The specimens were fixed in formalin, embedded in paraffin and used for immunohistochemistry. Histological grading was evaluated according to Hughes (1974) and the International Neuroblastoma Pathology Classification (INPC), established in 1999 and modified in 2003 (Hughes et al., 1974; Peuchmaur et al., 2003). A new histological entity was added recently (Tornoczky et al., 2007).

### Tissue-arrays

In order to study a broad range of adrenal tissue samples, we used the AD2081 adrenal-gland-disease-spectrum-tissue-array (US Biomax Inc., Rockville, MD), with 100 biopsies (200 cores). The tissue-array contains normal adrenal tissue as well as neuroblastomas and ganglioneuromas (n=4). WHO grading of the specimens was provided. The paraffin sections were used for immunohistochemistry as described below.

### Cell culture

The human NB cell lines SMS-Kan, SH-SY5Y and SK-N-AS (Reynolds et al., 1986) were maintained in a

## *EsVEGFR-2 in neuroblastoma*

humidified incubator at 37°C and 5% CO<sub>2</sub> atmosphere using RPMI 1640 medium (Lonza, Basel, Switzerland) with 10% fetal bovine serum (Biochrome, Berlin, Germany) and 1% penicillin/streptomycin (Invitrogen, Darmstadt, Germany). Human umbilical vein endothelial cells (HUVECs) and lymphatic endothelial cells (LECs; derived from lymphangiomas, see: Norgall et al., 2007) were cultured in endothelial cell growth medium (Lonza, Basel, Switzerland).

### *Induction of differentiation*

10<sup>6</sup> SMS-Kan, SK-SY5Y and SK-N-AS were seeded on 10 cm cell-culture dishes at day 0. They were allowed to adhere overnight. The next day (day 1) we started treatment with all-trans-retinoic acid (ATRA) dissolved in cell culture grade DMSO (Sigma, Taufkirchen, Germany). ATRA in DMSO was added to the RPMI to a final concentration of 5-10 μM. In control samples, the corresponding amount of pure DMSO was applied. At day 3, 6, 9 and 12 the medium was renewed and fresh ATRA or DMSO was added. Phase-contrast pictures were taken from all dishes at day 6, 9 and 12, and RNA was isolated.

### *RNA isolation from cultured NB cells*

Cells were rinsed twice with PBS and RNA was isolated directly from the culture plate using RNeasy-kit as recommended by the supplier (Qiagen, Hilden Germany). Quality of RNA samples was analyzed with NanoDrop spectrophotometer (NanoDrop products, Wilmington, DE) and ethidium bromide staining on agarose gels.

### *Real-time RT-PCR*

We prepared cDNA from 2 μg total RNA using Omniscript reverse transcriptase (Qiagen, Hilden, Germany). Real-time PCR was performed with an Opticon2 thermal cycler (MJ Research, Waltham, MA), using SYBR green JumpStart Taq ReadyMix (Sigma-Aldrich, Taufkirchen, Germany). For esVEGFR-2 the reverse primer recognizes the intron 13 motif, which is specific for the truncated transcript-variant of this secreted form of VEGFR-2 (Albuquerque et al., 2009). The probes were normalized using β-actin probes. Primers were: esVEGFR-2 fwd, 5'- GCCTTGCTC AAGACAGGAAG -3'; esVEGFR-2 rev, 5'- CAACT GCCTCTGCACAATGA -3'; β-actin fwd, 5'- GCATC CCCCAAAGTTCACAA -3'; β-actin rev, 5'- AGGAC TGGGCCATTCTCCTT -3'. Relative expression levels of transcripts were calculated with the ddCt-method using Microsoft Excel 2008 for Mac (Microsoft Corp. Redmond, WA).

### *Immunohistology*

Formalin fixed specimens were embedded in

paraffin. Sections of 5-7 μm were prepared for antigen retrieval as follows. After deparaffination, non-specific binding of antibodies was blocked with 1% BSA. Then, slides were incubated in citrate buffer (pH 6) and boiled in a microwave (5x5 min at 600W). After rinsing, sections were incubated for 10 min at 37°C with 0.1 % pepsin solution (Sigma, Deisenhofen, Germany). Primary anti-esVEGFR-2 polyclonal antibodies (esKDR, 102-PA19; Reliatech, Wolfenbüttel, Germany; antibodies generated against the specific C-terminal domain: CGRETILDHSAEAVGMP) were diluted 1:100. Secondary antibody was peroxidase-conjugated goat-anti-rabbit IgG (1:100, Sigma). DAB was used as chromogen and slides were counter-stained with nuclear-fast-red.

### *Western blot analyses*

To study the specificity of the anti-esVEGFR-2 polyclonal antibodies (Reliatech, Wolfenbüttel, Germany), we compared them with antibodies specific for the full-length form of the receptor (Reliatech; 101-M34). We used supernatants and lysates of three cell lines: HUVECs, LECs and the neuroblastoma cell line SK-N-AS. Cells were kept 48h in serum-free medium. Then, supernatants were collected and concentrated with Centricon centrifugal filter units (Biocompare), with a MW cut-off of 100 kDa. Cell lysates were prepared with standard lysis buffer. Supernatants and cell lysates were subjected to SDS-PAGE and blotted semi-dry on a PVDF membrane (Roth, Karlsruhe, Germany). Antibodies were blocked for 3 h in 5% milk powder in TBS with 0.02% Tween 20 (TBST). Primary antibodies were incubated over-night at 4°C in 5% milk powder in TBST. Primary antibodies were: anti-esVEGFR-2 polyclonal antibodies (dilution 1:1000) and anti-mbVEGFR-2 monoclonal antibodies (dilution 1:1000) and anti-β-actin monoclonal antibodies (Santa Cruz Biotechnology, CA; dilution 1: 1000). After rinsing twice in TBST, the secondary antibodies were applied for 1h at room temperature. Antibodies were: peroxidase-conjugated goat-anti-mouse IgG and peroxidase-conjugated goat-anti-rabbit IgG (Santa Cruz). Antibodies were detected using chemiluminescence detection kit (GE Healthcare, Little Chalfort, UK) and developed on X-ray film (Fuji Europe, Düsseldorf, Germany).

## **Results**

We intended to study immunolocalization of esVEGFR-2 in various human tissues. Since the antibody against the specific C-terminus of esVEGFR-2 has been produced only recently, we first studied its reactivity by Western blot analyses in comparison with an antibody, which detects the membrane-bound full-length receptor, mbVEGFR-2. We detected a specific double-band (due to different glycosylation) for mbVEGFR-2 in whole cell lysates of HUVECs and

### EsVEGFR-2 in neuroblastoma

LECs at appr. 210 kDa. No signal was found in the neuroblastoma (NB) cell line SK-N-AS (Fig. 1A). In concentrated supernatants of all three cell-lines a specific band for esVEGFR-2 was observed at appr. 115kDa (Fig. 1B). When esVEGFR-2 is produced in insect cells, the antibody produces a band at appr. 100 kDa (Reliatech, Wolfenbüttel, Germany), which indicates different glycosylation in insect cells. No signal was found in the lysates of our three cell lines (Fig. 1B). Cross reactivity of the esVEGFR-2 antibody with the mbVEGFR-2 was not observed.

Since NB is derived from the sympatho-adrenal system, we studied immunolocalization of esVEGFR-2 in the sympathetic trunk and the adrenal medulla of human embryos and fetuses. We observed a weak signal in the ganglia of the sympathetic trunk of 8 week-old embryos (Fig. 2A,B). In 11 week-old embryos staining was still weak, but some of the neurons were stronger positive (data not shown). In all embryos studied, a prominent signal was present in the adrenal medulla (Fig. 2C-E). The adrenal cortex was almost negative, except for some scattered cells which were positive (data not shown). In the dorsal root ganglia, a subpopulation of neurons expressed esVEGFR-2 (Fig. 2F). In the adrenal gland of a 5-month-old child (tissue-array AD2081) the expression pattern was basically the same as in the fetuses. The adrenal cortex was almost negative, whereas in the medulla numerous positive cells were found (Fig. 3).

The central nervous system (CNS) is free of lymphatics. However we hardly detected any staining in the neural parts of the brain, but found a clear signal in the epithelium of the choroid plexus (Fig. 4A,B). In the

developing spinal cord, the floor plate expressed esVEGFR-2, and, adjacent, the endothelium of the anterior spinal artery was positive (Fig. 4C), as were other arteries too (see below). Additionally, we observed esVEGFR-2 in the notochord, but not in the cartilage of the vertebral bodies (Fig. 4D).

Several other cell types expressed esVEGFR-2. The most prominent signal was found in cells of the hematopoietic system. These cells were located in the

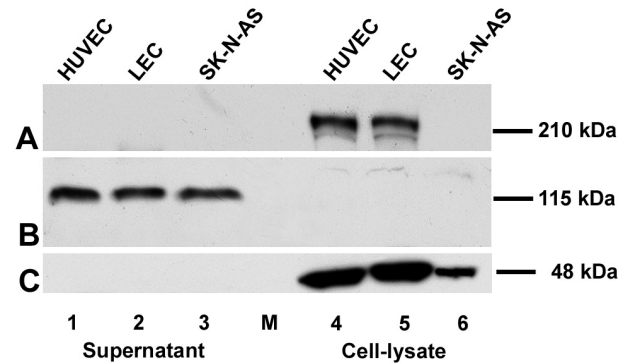


**Fig. 1.** Western blot analyses with antibodies against mbVEGFR-2 and esVEGFR-2. **A.** Anti-mbVEGFR-2 produces a specific band at 210 kDa in lysates of HUVECs and lymphangioma-derived LECs, but not in SK-N-AS or supernatants of the three cell lines. **B.** Anti-esVEGFR-2 produces a specific band at 115 kDa in the supernatant of all three cell lines, but not in cell-lysates. **C.** Loading of the gel was controlled with antibodies against  $\beta$ -actin. Lanes 1-3 contain supernatants; lanes 4-6 contain cell-lysates; M, lane of the size-marker.

**Table 1.** Anti-esVEGFR-2 immunoreactivity in human neuroblastoma.

No.	Internal No.	Grading	anti-esVEGFR2	Comment
1	#9246	3	±	almost all NB cells weakly stained
2	#9191	3	-	
3	#9208	3	-	
4	#0535	1	++	mainly in differentiating NB cells
5	#8417	2	-	
6	#8713	2	+	almost all NB cells stained
7	#5312	2	+	almost all NB cells stained
8	#3700	2	- [+]	some differentiating NB cells positive
9	#U5583	3	-	
10	#05583	3	-	
11	#5583S	3	-	
12	#4143	3	-	vascular cells positive
13	#8939	1	+	ganglioneuroblastoma and vascular cells positive
14	#7036	2	+	differentiating NB cells positive; regression
15	#1395	2	+	50% regression
16	#B5/6	III	-	
17	#B7/8	IV	-	
18	#B9/10	IV	-	
19	#B11/12	I	++	ganglioneuroma cells positive

19 specimens were evaluated. Pathology grade was determined according to Hughes et al. (1974) (grade 1-3) or the WHO grading (I-IV). Negative (-), weak (±), positive (+) and strongly positive (++) staining is demonstrated. Staining was found in more highly differentiated NB cells and in parts of the vascular system.

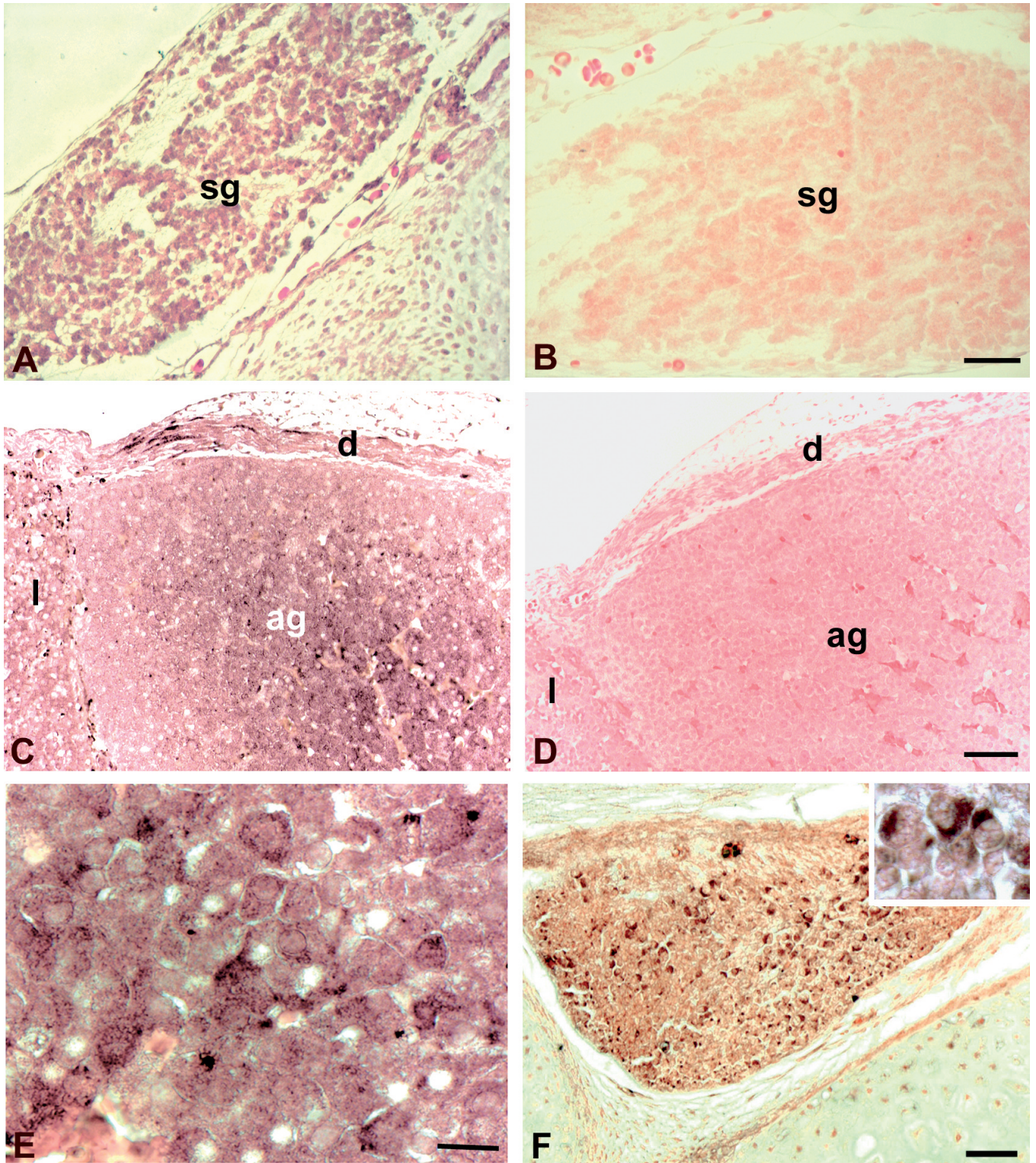


**Fig. 2.** Anti-esVEGFR-2 immunostaining of sympathetic tissues of human embryos. **A, B.** 8-week-old embryo. **C-E.** 10-week-old fetus. **F.** 11-weeks-old fetus. **A.** Expression in sympathetic ganglion (sg). **B.** Negative control of the specimen in **A.** **C.** Expression in medulla of adrenal gland (ag); l, liver; d, diaphragm. **D.** Negative control of the specimen in **C.** **E.** Higher magnification of **C** showing adrenal medulla. **F.** Expression in neurons of a dorsal root ganglion. Insert: Higher magnification of neurons. Bars: A-D, F, 160  $\mu$ m; E, 20  $\mu$ m.

circulating blood or in the soft connective tissue such as the adventitia of the portal vein (Fig. 5A,B). Within the liver, hematopoietic cells were strongly positive, whereas hepatocytes showed a weak signal (Fig. 5C). Besides hematopoietic cells, endothelial cells expressed esVEGFR-2. The signal was not present in all endothelial cells but was restricted to specific parts of the vascular tree. It was mostly confined to arterial endothelium such as the intercostal arteries (Fig. 5D) or the anterior spinal artery (Fig. 4C). In accordance with previous studies on the foreskin of infants (Pavlakovic et al., 2010), we found esVEGFR-2 in the immature epidermis of fetuses (Fig. 6A,B). Additionally, we observed esVEGFR-2 expression in skeletal muscle such as the diaphragm (Fig. 2C). Interestingly, the signal was strongest in the peripheral parts of the muscle fibres adjacent to the insertions of the tendons (Fig. 6C). In the mucous membrane of the gut we found esVEGFR-2 in the epithelium and in scattered leukocytes in the lamina propria (Fig. 6D).

Although the number of primary NB in this study was relatively small (n=19), it became evident that esVEGFR-2 expression was higher in differentiating lesions (Table 1; Fig. 7A-D). In highly malignant tumours (Hughes grade 3 and WHO grading III, IV) we

only found one specimen with weak esVEGFR-2 expression. Highest expression was found in Hughes grade 1 NB, mainly in differentiating NB cells (Table 1). In the differentiating type of NB, we observed clear expression in the cytoplasm of maturing neuroblasts, whereas in the undifferentiated type esVEGFR-2 was hardly detectable (Fig. 7A-C). Furthermore, in ganglioneuroblastoma and in ganglioneuroma (Hughes grade 1) the majority of perikarya of ganglion cells were esVEGFR-2-positive (Fig. 7D). Again, this suggests that mature sympathetic ganglion cells, or at least a subpopulation of them, function as inhibitors of lymphangiogenesis. Additionally, in some specimens esVEGFR-2 expression was observed in parts of the tumour vascular system. Both endothelial cells and smooth muscle cells were positive (data not shown).

All-trans retinoic acid (ATRA) has often been used *in vitro* for the induction of NB cell differentiation (Reynolds et al., 2003). We treated the NB cell line SMS-Kan with 5  $\mu$ M and 10  $\mu$ M ATRA (dissolved in DMSO), or solvent alone, for 6, 9 and 12 days. During the treatment of the cells, their phenotype changed characteristically from round and cloddy to slender. The differentiated cells possessed long, neuron-like extensions (Fig. 8A,B). We quantified esVEGFR-2

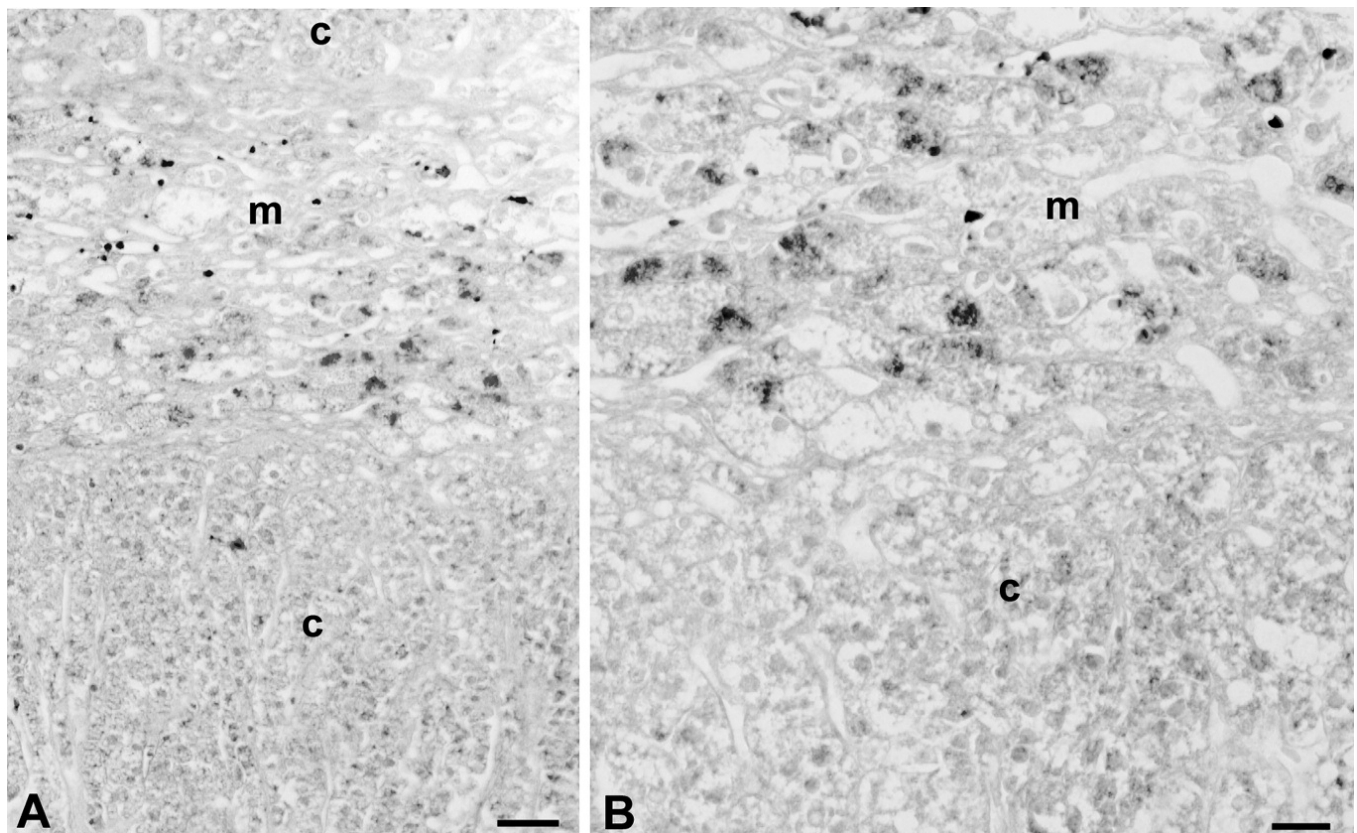


**Fig. 3.** Anti-esVEGFR-2 immunostaining of the adrenal gland of a 5-month-old child. **A.** Overview showing adrenal cortex (c) and adrenal medulla (m). **B.** Higher magnification showing esVEGFR-2-positive cells in the adrenal medulla. Bars: A, 100  $\mu$ m; B, 50  $\mu$ m.

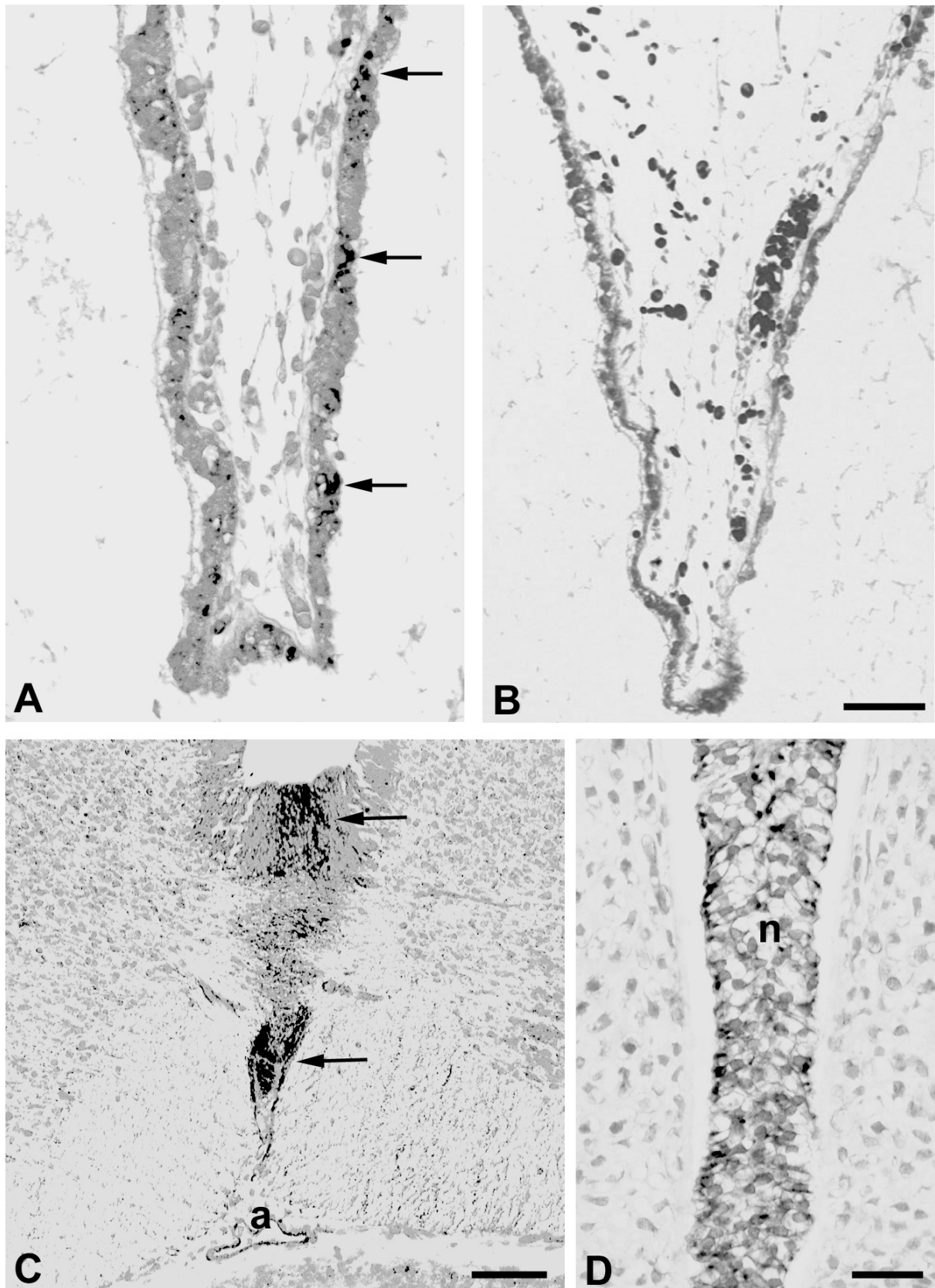


**Fig. 4.** Anti-esVEGFR-2 immunostaining of the CNS and notochord of human embryos. **A-D.** 8-week-old embryo. **A.** Expression (arrows) in the epithelium of the choroid plexus. **B.** Negative control of the specimen in **A.** **C.** Expression (arrows) in the floor plate of the neural tube and in the anterior spinal artery (a). **D.** Expression in the notochord (n). Bars: A, B, 100  $\mu$ m; C, 200  $\mu$ m; D, 80  $\mu$ m.

mRNA expression by real-time RT-PCR and observed a considerable increase after 6, 9 and 12 days of treatment (Fig. 8C). We also performed ATRA treatment on SH-SY5Y and SK-N-AS. In SH-SY5Y we observed a marked increase in esVEGFR-2 expression after 6 days as compared to day 0. This, however, was not significantly different from the DMSO controls. In SK-N-AS we did not observe any regulation of esVEGFR-2 after 6 days (data not shown). Therefore, only a subset of NB cell lines seems to be suitable to recapitulate the *in vivo* results. The highly heterogeneous reactivity of the cell lines towards ATRA treatment also became evident in our global transcriptome analyses (data not shown).

### Discussion

It has been known for quite some time that

hemangiogenesis is regulated by activators as well as inhibitors. Activators of lymphangiogenesis (VEGF-C, VEGF-D) were detected several years ago (Jeltsch et al., 1997; Oh et al., 1997; Achen et al., 1998). However, an endogenous inhibitor of lymphangiogenesis (esVEGFR-2) has been detected only recently (Albuquerque et al., 2009). Here, we studied expression of esVEGFR-2 at protein level. First we verified the specificity of the polyclonal antibodies against esVEGFR-2, which detect a band at 115 kDa in the supernatants of HUVECs, lymphangioma LECs and SK-N-AS, a human neuroblastoma (NB) cell line. In a control experiment, antibodies against the membrane-bound VEGFR-2 (mbVEGFR-2) produce a double-band at 210 kDa in whole cell lysates of HUVECs and LECs, but not SK-N-AS.

The mbVEGFR-2 consists of 1375aa with a

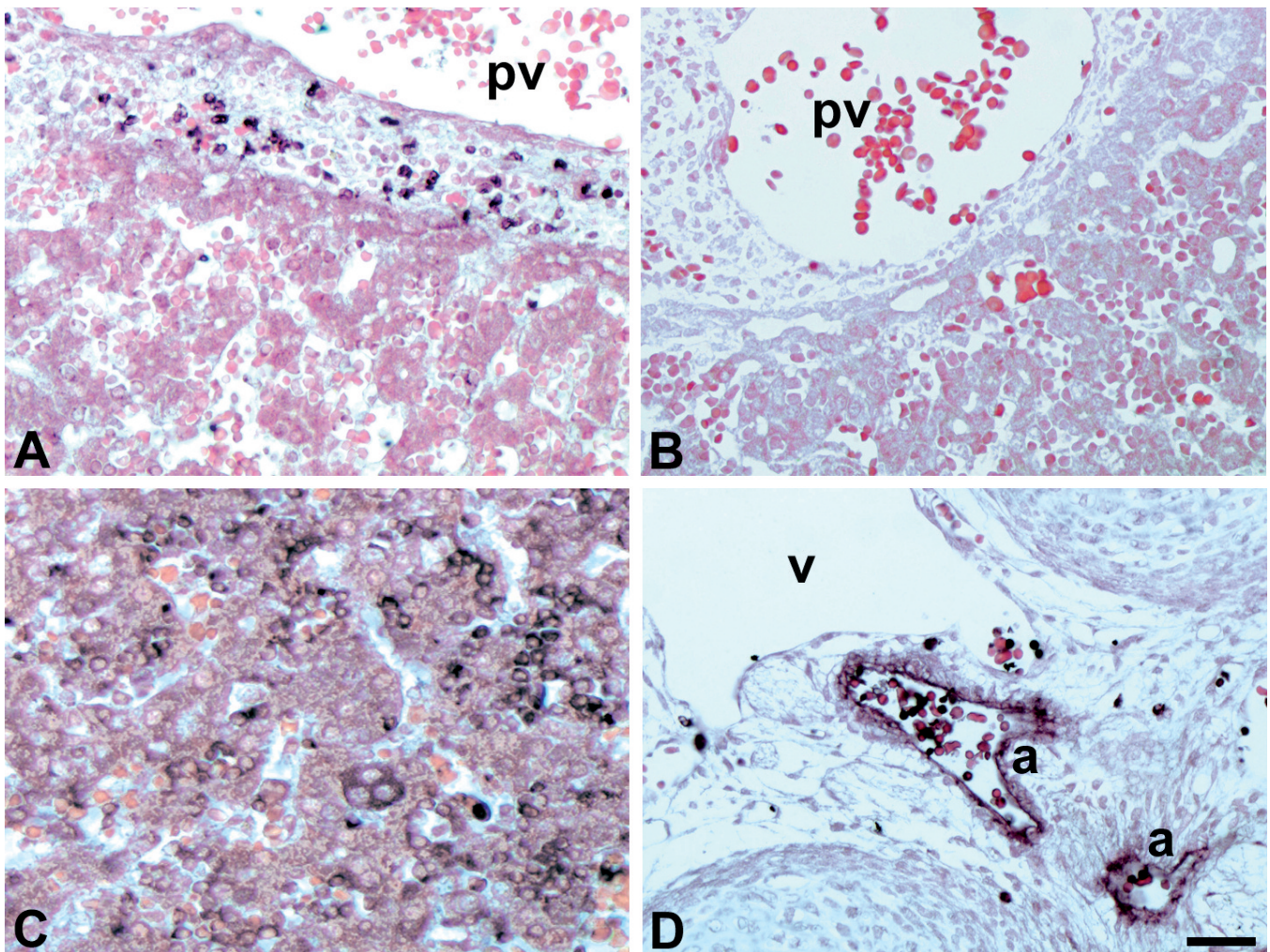


**Fig. 5.** Anti-esVEGFR-2 immunostaining of hematopoietic and endothelial cells in human embryos. **A-C.** 8-week-old embryo. **D.** 10-week-old embryo. **A.** Expression in scattered cells in the adventitia of the portal vein (pv) in the liver. **B.** Negative control of the specimen in **A.** **C.** Expression in hematopoietic cells in the liver. Weak expression in hepatocytes. **D.** Expression in the endothelium of segmental arteries (a), but not in veins (v), and in scattered cells in the soft connective tissue. Bars: A-D, 60  $\mu\text{m}$ .



### *EsVEGFR-2 in neuroblastoma*

theoretical weight of appr. 152 kDa, but due to glycosylation the receptor runs at ~210 kDa and displays a double band as shown here. The soluble splice variant of esVEGFR-2 consists of 659aa with a theoretical weight of appr. 74 kDa, and again, glycosylation seems to increase size by ~40 kDa. We have previously shown at RNA level that SK-N-AS produce esVEGFR-2, but not mbVEGFR-2 (Becker et al., 2010). Here, we have confirmed this finding at protein level. Blood vascular and lymphatic endothelial cells typically express mbVEGFR-2. The expression of esVEGFR-2 in HUVECs could have been expected on the basis of previous data (Albuquerque et al., 2009; Pavlakovic et al., 2010). The expression of esVEGFR-2 in LECs may be surprising, although it has to be considered that our LECs are derived from lymphangiomas, which show an abnormally high expression of VEGFR-3 as compared to normal LECs (Norgall et al., 2007). Therefore, esVEGFR-2 may also be expressed abnormally highly in these cells. The antibody against esVEGFR-2 does not cross-react with mbVEGFR-2 and can therefore be considered a reliable tool.

#### *EsVEGFR-2 in human embryos*

The expression of esVEGFR-2 has not yet been

studied in human embryos and fetuses at protein level. In neonatal foreskin, we have previously shown that it is located in the epidermis and in blood vascular endothelium (Pavlakovic et al., 2010). It is also found in the corneal epithelium of humans and mice, and inhibits ingrowth of lymphatics into the murine corneal stroma (Albuquerque et al., 2009). In mouse, Northern blot analyses have shown that esVEGFR-2 is highly expressed in embryos, and in adult organs such as lung, kidney and heart, but only low in brain, liver, spleen, thymus, testis and ovary (Albuquerque et al., 2009). Here, we studied paraffinated sections of human embryos and fetuses and used antigen retrieval techniques in combination with specific esVEGFR-2 antibodies. We show weak expression in sympathetic ganglia and strong expression in the adrenal medulla, which are the tissues that can give rise to NB. In 18 week-old human fetuses there are no lymphatics in the adrenal glands (Jin et al., 2010), which may be due to the high expression of esVEGFR-2 in the adrenal medulla. In accordance with previous studies on human and mouse tissues (Albuquerque et al., 2009; Pavlakovic et al., 2010), we observed esVEGFR-2 in the epidermis and in blood vascular endothelial cells, mainly those of arteries. Additionally, we detected a number of expression sites that have not been described before. The

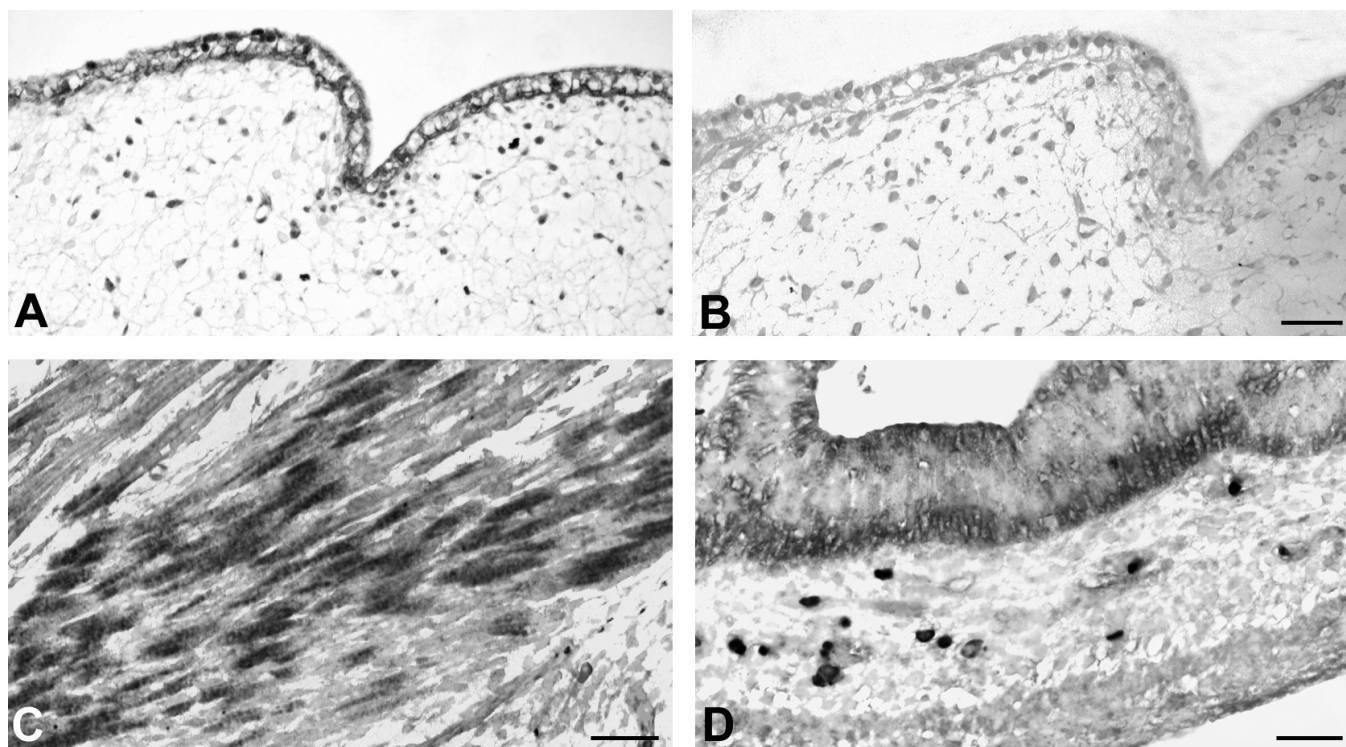


**Fig. 6.** Anti-esVEGFR-2 immunostaining of various tissues of human embryos. **A, B.** 8-week-old embryo. **C, D.** 10-week-old fetus **A.** Expression in epidermis and in scattered cells of the dermis. **B.** Negative control of the specimen in **A.** **C.** Expression in skeletal muscle. **D.** Expression in gut epithelium and in scattered cells in the mucous membrane. Bars: **A, B,** 80  $\mu$ m; **C, D,** 60  $\mu$ m.

strongest signal was found in hematopoietic cells of the fetal liver, while the adjacent hepatocytes only showed a weak signal. Blood cells and scattered leukocytes in the soft connective tissues of the mucous membranes and the adventitia of blood vessels also express esVEGFR-2. This strongly indicates that leukocytes control lymphangiogenesis both negatively but also positively by the expression of VEGF-C (Ji, 2007). The loss of esVEGFR-2 in leukocytes may induce hyperproliferation of lymphatics, which may then give rise to abnormal lympho-venous connections and embryonic lethality. This phenomenon has been observed in a number of leukocyte-specific transgenic mice, such as the tyrosine kinase Syk null-mice (Böhmer et al., 2010).

The CNS does not contain lymphatics, and we had expected stronger expression of esVEGFR-2 in it. However, we observed esVEGFR-2 in the choroid

plexus, and it is likely that there are sufficient amounts of this inhibitor in the cerebrospinal fluid to prevent lymphangiogenesis into the CNS. Additionally, there is esVEGFR-2 expression in two strategically important sites, the floor plate and the dorsal root ganglia. During development, blood vessels enter the neural tube immediately adjacent to the floor plate, which is most likely induced by VEGF-A (Wilting and Christ, 1996). It appears that esVEGFR-2 expression simultaneously prevents ingrowth of lymphatics into this 'vulnerable' site. Comparably, the esVEGFR-2-positive dorsal root ganglia are located at the bottleneck between the CNS and the extra-dural mesenchyme.

We observed expression of esVEGFR-2 in the epidermis, which is in line with previous studies on humans and mice (Pavlakovic et al., 2010; Albuquerque et al., 2009). In mice, knock-out of esVEGFR-2 in the

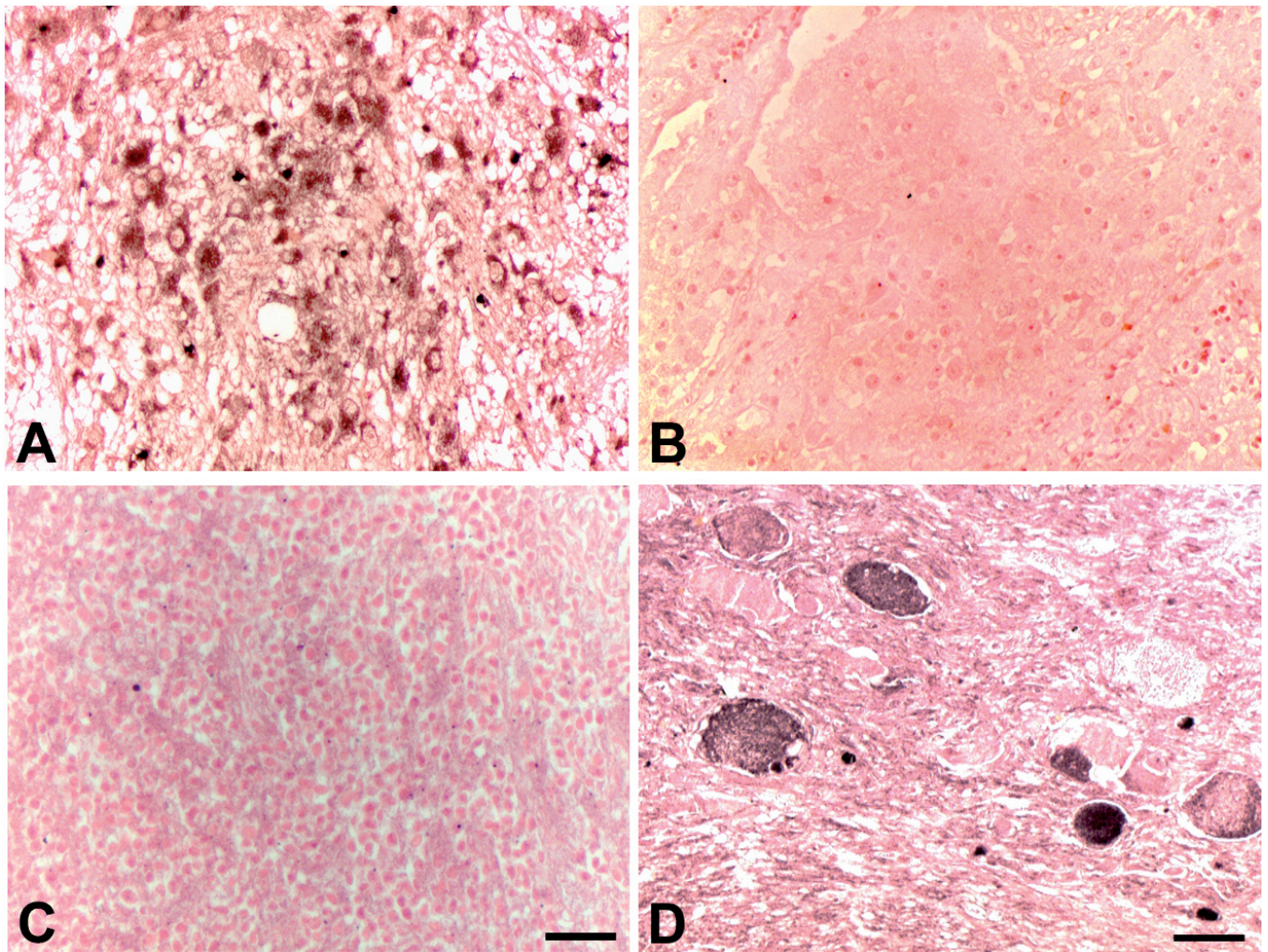


**Fig. 7.** Anti-esVEGFR-2 immunostaining of primary neuroblastoma and ganglioneuroma. **A.** Differentiating type of neuroblastoma showing esVEGFR-2 in the cytoplasm of maturing neuroblasts. **B.** Negative control of the specimen shown in **A.** **C.** Undifferentiated type of neuroblastoma. EsVEGFR-2 is almost undetectable. **D.** A subpopulation of ganglion cells expresses esVEGFR-2 in ganglioneuroma. Bars: A-C, 90  $\mu$ m; D, 60  $\mu$ m.

## EsVEGFR-2 in neuroblastoma

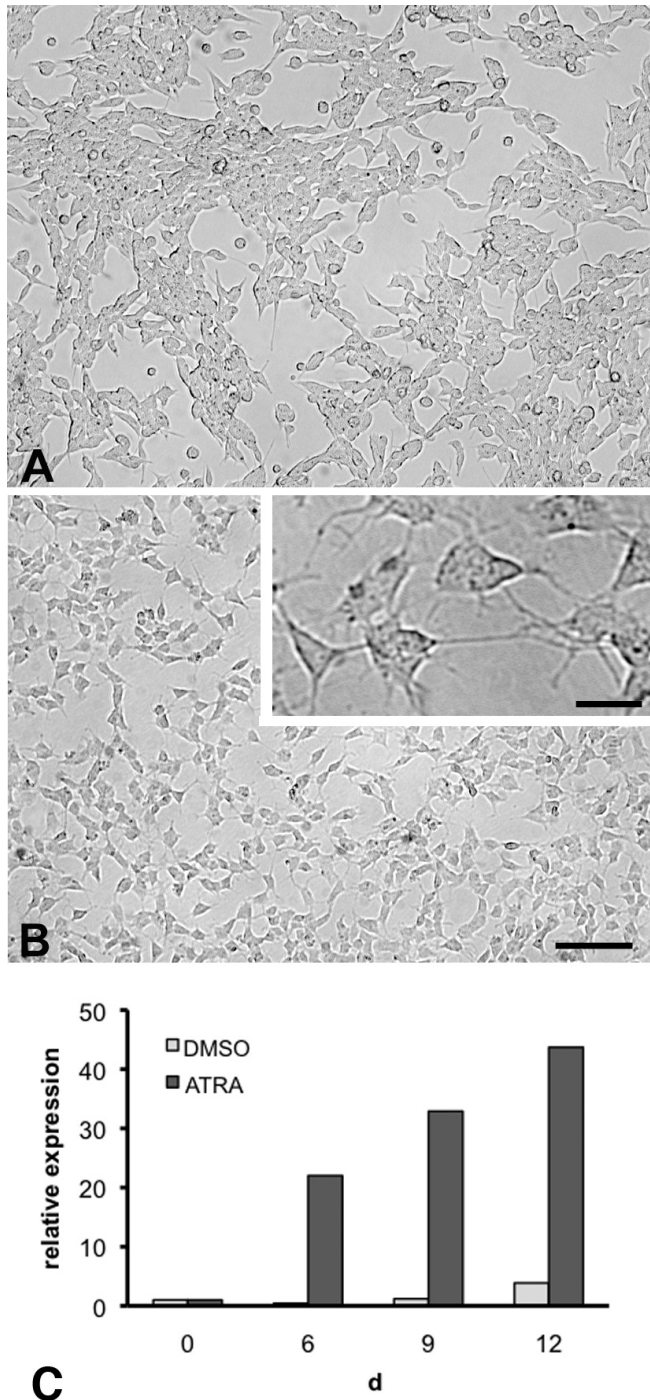


**Fig. 8.** Relative esVEGFR-2 mRNA expression in SMS-Kan differentiated 5 $\mu$ M ATRA. Phase-contrast images of SMS-Kan treated with solvent alone (A) or 5  $\mu$ M ATRA (B). ATRA-treated cells have a slender morphology with filopodial extensions. Insert: Note neuronal morphology of cells. C. Real-time RT-PCR analyses of differentiated and solvent treated cells. Relative expression at day 0 was set as 1. Note the significant increase in expression on days 6, 9 and 12. A slight increase can also be seen in the DMSO controls. A representative experiment is shown. Bars: A, B, 120  $\mu$ m; Insert B, 25  $\mu$ m.

epidermis induces hyperplasia of dermal lymphatics, and it is likely that the skin, due to its great surface, is the largest source for this inhibitor. Additionally we found esVEGFR-2 in skeletal muscle and gut epithelium, and it will be of interest if tissue specific knock-outs have similar effects as those in epidermis.

### EsVEGFR-2 in neuroblastoma

Staging of neuroblastoma (NB) is related to its interactions with the lymphovascular system. According to the International Neuroblastoma Staging System (INSS), stage 1 and 2 NBs are localized tumours, and lymph nodes are microscopically negative in stage 1 (Brodeur et al., 1988). Stage 2 shows some degree of heterogeneity. Whereas in stage 2A lymph nodes are negative, in stage 2B ipsilateral nodes are positive. Stage 3 either shows involvement of contralateral nodes or infiltrating growth across the midline. Metastasis into systemic lymph nodes, bone marrow, liver and other organs is characteristic of stage 4 NB (Brodeur et al., 1993). Despite the highly heterogeneous behaviour, interactions with the lymphatics seem to be a frequent phenomenon in NB.

Active interactions of tumours with the lymphatics have long been denied, mainly because a functional lymphatic system has not been found in tumours (Tanigawa et al., 1981; Jain, 1987; Zeidman et al., 1955). However, already some decades ago, dilated lymphatics were observed at the invasive front of breast cancer (Lee et al., 1990; Cann et al., 1995). In recent years, a number of groups have studied the relationship between the lymphangiogenic growth factors VEGF-C or VEGF-D and lymphatic invasion or lymph node metastases in human tumours (Tammela and Alitalo, 2010; Pepper et al., 2003). A significant correlation between tumour VEGF-C levels and lymph node metastasis was found in most of these studies, e.g. in thyroid carcinoma, esophageal squamous cell carcinoma, cervical, pancreatic and endometrial carcinoma, gallbladder cancer, ovarian and prostatic carcinoma as well as head and neck squamous cell carcinoma (Pepper et al., 2003). In other types of cancer the same positive correlation was found, but a minority of studies showed that this is not always true, e.g. in gastric and breast carcinoma, mesothelioma, lung and colorectal carcinoma.

Of interest for our study, Komuro and coworkers did not observe a positive correlation between VEGF-C levels and lymph node metastasis in NB (Komuro et al., 2001). This was contradicted by a recent study where VEGF-C was identified as a risk factor in stage 4 NB (Nowicki et al., 2008). The existence of lymphatics in some NB specimens has been shown before (Lagodny et al., 2007). Discrepancies may be explained by the fact that inhibitors of VEGF-C signaling were not taken into account. EsVEGFR-2 inhibits VEGF-C signalling and lymphangiogenesis via decrease of VEGFR-3 activity (Albuquerque et al., 2009). We have recently

investigated the mRNA expression of various VEGFs and their receptors in primary NB from a cohort of 49 patients (of stages 1, 2, 3, 4 and 4s), which were not treated by radio- or chemotherapy prior to resection (Becker et al., 2010). We did not detect significant regulation of VEGFs and their membrane-bound receptors, but observed significant down-regulation of esVEGFR-2 in stages 3, 4 and 4s as compared to stages 1 and 2.

Here, we provide further evidence that the behaviour of NB may be regulated by esVEGFR-2. In primary NB, there is a clearer signal in low grade, differentiating types. We found immunostaining in the cytoplasm of neuroblasts from differentiating NB and in perikarya of differentiated neurons in ganglioneuroblastoma and ganglioneuroma. In contrast, undifferentiated grade 3 NB are almost negative for esVEGFR-2. In addition to the tumour cells, parts of the vascular system (endothelial as well as smooth muscle cells) can express esVEGFR-2. Our *in vitro* studies support the immunohistological observations. Of three NB cell lines tested (SMS-Kan, SH-SY5Y and SK-N-AS) induction of differentiation in SMS-Kan with 5  $\mu$ M and 10  $\mu$ M ATRA results in massive up-regulation of esVEGFR-2 mRNA. The most significant increase, as compared to the DMSO controls, can be seen after 6 days of induction, whereas after 9 and 12 days the increase becomes relatively smaller, indicating some kind of adaptation over time. This might be due to the fact that ATRA can be stored intracellularly (Lane and Bailey, 2005).

In summary, we show that esVEGFR-2 is expressed in sympathetic ganglia and adrenal medulla of human embryos and fetuses. It is highly expressed in the cytoplasm of differentiating neuroblasts and seems to correlate with the grading of NB. As shown previously, it is significantly lower in progressed NB stages (Becker et al., 2010), which regularly show lymph node involvement. Because VEGF-C is almost equally expressed in all NB stages, we suggest that the balance between activators and inhibitors of lymphangiogenesis is mainly regulated by esVEGFR-2, or by VEGF-D. Lymphangiogenesis can obviously be induced in progressed and undifferentiated NB by the down-regulation of esVEGFR-2, which in turn may promote lymphogenic metastasis. Expression of esVEGFR2 seems to be a sign for differentiation in sympathetic cells. Our data suggest that lymphangiogenesis is regulated in various types of tissues by both activators and inhibitors, and the balance between the two must be tightly controlled.

---

**Acknowledgements.** We thank Mrs. S. Schwoch, Mr. B. Manshausen and Mr. F. Ludewig for their excellent technical assistance, and Drs. Frank Berthold, Barbara Hero and Jessica Theissen (German Neuroblastoma Studies Group, Children's Hospital University Cologne, Cologne, Germany) for providing tumour samples and data. The study was supported by a grant from the Deutsche Forschungsgemeinschaft (Wi 1452/11-1).

---

## References

- Achen M.G., Jeltsch M., Kukk E., Makinen T., Vitali A., Wilks A.F., Alitalo K. and Stacker S.A. (1998). Vascular endothelial growth factor D (VEGF-D) is a ligand for the tyrosine kinases VEGF receptor 2 (Flk1) and VEGF receptor 3 (Flt4). *Proc. Natl. Acad. Sci. USA* 95, 548-553.
- Albuquerque R.J., Hayashi T., Cho W.G., Kleinman M.E., Dridi S., Takeda A., Baffi J.Z., Yamada K., Kaneko H., Green M.G., Chappell J., Wilting J., Weich H.A., Yamagami S., Amano S., Mizuki N., Alexander J.S., Peterson M.L., Brekken R.A., Hirashima M., Capoor S., Usui T., Ambati B.K. and Ambati J. (2009). Alternatively spliced vascular endothelial growth factor receptor-2 is an essential endogenous inhibitor of lymphatic vessel growth. *Nat. Med.* 15, 1023-1030.
- Becker J., Pavlakovic H., Ludewig F., Wilting F., Weich H.A., Albuquerque R., Ambati J. and Wilting J. (2010). Neuroblastoma progression correlates with downregulation of the lymphangiogenesis inhibitor sVEGFR-2. *Clin. Cancer Res.* 16, 1431-1441.
- Böhmer R., Neuhaus B., Bühren S., Zhang D., Stehling M., Böck B. and Kiefer F. (2010). Regulation of developmental lymphangiogenesis by syk(+) leukocytes. *Dev. Cell.* 18, 437-449.
- Brodeur G.M., Seeger R.C., Barrett A., Berthold F., Castleberry R.P., D'Angio G., De Bernardi B., Evans A.E., Favrot M., Freeman A.I., Haase G., Hartmann O., Hayes F.A., Helson L., Kemshead J., Lampert F., Ninane J., Ohkawa H., Philip T., Pinkerton C.R., Pritchard J., Sawada T., Siegel S., Smith E.I., Tsuchida Y. and Voute P.A. (1988). International criteria for diagnosis, staging, and response to treatment in patients with neuroblastoma. *J. Clin. Oncol.* 6, 1874-1881.
- Brodeur G.M., Pritchard J., Berthold F., Carlsen N.L., Castel V., Castleberry R.P., De Bernardi B., Evans A.E., Favrot M., Hedborg F., Kaneko M., Kamshead J., Lampert F., Lee R.E.J., Look A.T., Pearson A.D.J., Philip T., Roald B., Sawada T., Seeger R.C., Tsuchida Y. and Voute P.A. (1993). Revisions of the international criteria for neuroblastoma diagnosis, staging, and response to treatment. *J. Clin. Oncol.* 11, 1466-1477.
- Cann S.A., van Netten J.P., Ashby T.L., Ashwood-Smith M.J. and van der Westhuizen N.G. (1995). Role of lymphagenesis in neovascularisation. *Lancet* 346, 903.
- Ebos J.M., Bocci G., Man S., Thorpe P.E., Hicklin D.J., Zhou D., Jia X. and Kerbel R.S. (2004). A naturally occurring soluble form of vascular endothelial growth factor receptor 2 detected in mouse and human plasma. *Mol. Cancer Res.* 2, 315-326.
- Folkman J. (1996). Angiogenesis and tumor growth. *N. Engl. J. Med.* 334, 921.
- Hughes M., Marsden H.B. and Palmer M.K. (1974). Histologic patterns of neuroblastoma related to prognosis and clinical staging. *Cancer* 34, 1706-1711.
- Jain R.K. (2007). Transport of molecules in the tumor interstitium: a review. *Cancer Res.* 47, 3039-3051.
- Jeltsch M., Kaipainen A., Joukov V., Meng X., Lakso M., Rauvala H., Swartz M., Fukumura D., Jain R.K. and Alitalo K. (1997). Hyperplasia of lymphatic vessels in VEGF-C transgenic mice. *Science* 276, 1423-1425.
- Ji R.C. (2007). Lymphatic endothelial cells, inflammatory lymphangiogenesis, and prospective players. *Curr. Med. Chem.* 14, 2359-2368.
- Jin Z.W., Nakamura T., Yu H.C., Kimura W., Murakami G. and Cho B.H.

*EsVEGFR-2 in neuroblastoma*

- (2010). Fetal anatomy of peripheral lymphatic vessels: a D2-40 immunohistochemical study using a 18-week human fetus (CRL 155 mm). *J. Anat.* 216, 671-682.
- Karpanen T., Egeblad M., Karkkainen M.J., Kubo H., Yla-Herttuala S., Jaattela M. and Alitalo K. (2001). Vascular endothelial growth factor C promotes tumor lymphangiogenesis and intralymphatic tumor growth. *Cancer Res.* 61, 1786-1790.
- Komuro H., Kaneko S., Kaneko M. and Nakanishi Y. (2001). Expression of angiogenic factors and tumor progression in human neuroblastoma. *J. Cancer Res. Clin. Oncol.* 127, 739-743.
- Lagodny J., Juttner E., Kayser G., Niemeyer C.M. and Rossler J. (2007). Lymphangiogenesis and its regulation in human neuroblastoma. *Biochem. Biophys. Res. Commun.* 352, 571-577.
- Lane M.A. and Bailey S.J. (2005). Role of retinoid signalling in the adult brain. *Prog. Neurobiol.* 75, 275-293.
- Lee A.K., DeLellis R.A., Silverman M.L., Heatley G.J. and Wolfe H.J. (1990). Prognostic significance of peritumoral lymphatic and blood vessel invasion in node-negative carcinoma of the breast. *J. Clin. Oncol.* 8, 1457-1465.
- Meitar D., Crawford S.E., Rademaker A.W. and Cohn S.L. (1996). Tumor angiogenesis correlates with metastatic disease, N-myc amplification, and poor outcome in human neuroblastoma. *J. Clin. Oncol.* 14, 405-414.
- Norgall S., Papoutsis M., Rossler J., Schweigerer L., Wilting J. and Weich H.A. (2007). Elevated expression of VEGFR-3 in lymphatic endothelial cells from lymphangiomas. *BMC Cancer* 7, 105.
- Nowicki M., Konwerska A., Ostalska-Nowicka D., Derwich K., Miskowiak B., Kondraciuk B., Samulak D. and Witt M. (2008). Vascular endothelial growth factor (VEGF)-C - a potent risk factor in children diagnosed with stadium 4 neuroblastoma. *Folia Histochem. Cytobiol.* 46, 493-499.
- O'Rahilly R.M. and Müller F. (1996). Human embryology and teratology. 2nd ed. Wiley-Liss. Inc. New York, N.Y.
- Oh S.J., Jeltsch M.M., Birkenhager R., McCarthy J.E., Weich H.A., Christ B., Alitalo K. and Wilting J. (1997). VEGF and VEGF-C: specific induction of angiogenesis and lymphangiogenesis in the differentiated avian chorioallantoic membrane. *Dev. Biol.* 188, 96-109.
- Papoutsis M., Siemeister G., Weindel K., Tomarev S.I., Kurz H., Schachtele C., Martiny-Baron G., Christ B., Marme D. and Wilting J. (2000). Active interaction of human A375 melanoma cells with the lymphatics in vivo. *Histochem. Cell Biol.* 114, 373-385.
- Pavlakovic H., Becker J., Albuquerque R., Wilting J. and Ambati J. (2010). Soluble VEGFR-2: an antilymphangiogenic variant of VEGF receptors. *Ann. NY Acad. Sci.* 1207 Suppl. 1, E7-15.
- Pepper M.S., Tille J.C., Nisato R. and Skobe M. (2003). Lymphangiogenesis and tumor metastasis. *Cell Tissue Res.* 314, 167-177.
- Peuchmaur M., d'Amore E.S., Joshi V.V., Hata J., Roald B., Dehner L.P., Gerbing R.B., Stram D.O., Lukens J.N., Matthay K.K. and Shimada H. (2003). Revision of the International Neuroblastoma Pathology Classification: confirmation of favorable and unfavorable prognostic subsets in ganglioneuroblastoma, nodular. *Cancer* 98, 2274-2281.
- Reynolds C.P., Biedler J.L., Spengler B.A., Reynolds D.A., Ross R.A., Frenkel E.P. and Smith R. G. (1986). Characterization of human neuroblastoma cell lines established before and after therapy. *J. Natl. Cancer Inst.* 76, 375-387.
- Reynolds C.P., Matthay K.K., Villablanca J.G. and Maurer B.J. (2003). Retinoid therapy of high-risk neuroblastoma. *Cancer Lett.* 197, 185-192.
- Roeckl W., Hecht D., Sztajer H., Waltenberger J., Yayon A. and Weich H.A. (1998). Differential binding characteristics and cellular inhibition by soluble VEGF receptors 1 and 2. *Exp. Cell Res.* 241, 161-170.
- Rossler J., Taylor M., Georger B., Farace F., Lagodny J., Peschka-Suss R., Niemeyer C.M. and Vassal G. (2008). Angiogenesis as a target in neuroblastoma. *Eur. J. Cancer* 44, 1645-1656.
- Shibata M.A., Ambati J., Shibata E., Albuquerque R.J., Morimoto J., Ito Y. and Otsuki Y. (2010). The endogenous soluble VEGF receptor-2 isoform suppresses lymph node metastasis in a mouse immunocompetent mammary cancer model. *BMC Med.* 8, 69.
- Skobe M., Hawighorst T., Jackson D.G., Prevo R., Janes L., Velasco P., Riccardi L., Alitalo K., Claffey K. and Detmar M. (2001). Induction of tumor lymphangiogenesis by VEGF-C promotes breast cancer metastasis. *Nat. Med.* 7, 192-198.
- Stacker S.A., Caesar C., Baldwin M.E., Thornton G.E., Williams R.A., Prevo R., Jackson D.G., Nishikawa S., Kubo H. and Achen M.G. (2001). VEGF-D promotes the metastatic spread of tumor cells via the lymphatics. *Nat. Med.* 7, 186-191.
- Tammela T. and Alitalo K. (2010). Lymphangiogenesis: Molecular mechanisms and future promise. *Cell* 140, 460-476.
- Tanigawa N., Kanazawa T., Satomura K., Hikasa Y., Hashida M., Muranishi S. and Sezaki H. (1981). Experimental study on lymphatic vascular changes in the development of cancer. *Lymphology* 14, 149-154.
- Tornoczky T., Semjen D., Shimada H. and Ambros I.M. (2007). Pathology of peripheral neuroblastic tumors: significance of prominent nucleoli in undifferentiated/poorly differentiated neuroblastoma. *Pathol. Oncol. Res.* 13, 269-275.
- Weiss W.A., Aldape K., Mohapatra G., Feuerstein B.G. and Bishop J.M. (1997). Targeted expression of MYCN causes neuroblastoma in transgenic mice. *EMBO J.* 16, 2985-2995.
- Wilting J. and Christ B. (1996). Embryonic angiogenesis: a review. *Naturwissenschaften* 83, 153-164.
- Zeidman I., Copeland B.E. and Warren S. (1955). Experimental studies on the spread of cancer in the lymphatic system. II. Absence of a lymphatic supply in carcinoma. *Cancer* 8, 123-127.